Riley Starling

Constructing a Model Population of Supermassive Black Hole Binaries from the Horizon Run 5 Simulation using Holodeck

Submitted in accordance with the
requirements for completion of the degree of
Bachelor of Science in Physics

submitted to
Haverford College

Supervisor
Prof. Andrea Lommen

Department of Physics and Astronomy
Chair: Prof. Karen Masters

370 Lancaster Ave
Haverford PA 19041

May 2024

ABSTRACT

Current research in gravitational wave detection has included supermassive black hole binary (SMBHB) populations from a limited number of cosmological simulations. This research has yet to be done with the Horizon Run 5 (HR5) simulation. Extracting a list of SMBHBs from HR5 allows us to begin construction on a realistic data set that will be used for a variety of studies, for example, testing the sensitivity of detection software Enterprise to different aspects of the population. To prepare the population from HR5, the black hole synthesis software Holodeck is used to model the binary's evolution until coalescence. This population is then resampled, expanding the data set into a representation of the full observer-frame universe. This observer-frame population is further improved by redistributing the evolved binaries across orbital frequency bins based on a power law with a spectral index of $-8/3$. The resulting set of binaries has a redshift range of $0.28 < z < 1.91$, which is suitable for simulating a detectable gravitational wave background.

Contents

1. INTRODUCTION

Gravitational wave (GW) detection research often tests signals simulated by supermassive black hole (SMBH) populations extracted from a cosmological simulation, yet there is limited diversity in the types of simulations used. For instance, Horizon Run 5 (HR5) is a hydrodynamical cosmological simulation that has not been utilized in these types of studies until now. This paper outlines how we developed a population of supermassive black hole binaries (SMBHBs) from HR5 into a data set that is suitable for future gravitational wave detection experiments.

Accepted by the scientific community to be at the center of almost every galaxy, SMBHs are the largest type of black hole (BH), with masses $M_{\bullet} \sim 10^6 - 10^{10} M_{\odot}$ (Sobolenko, M. et al. 2021). The Milky Way has an SMBH called Sagittarius-A* at its center with a mass of around $2.6 \times 10^6 M_{\odot}$ (Ghez et al. 1998). Black holes have the potential to merge with one another by forming an SMBHB and colliding into one body once they are sufficiently bound (Begelman et al. 1980).

The formation of these SMBHBs begins with a galaxy merger. The SMBHs that were once the center of the two galaxies fall into the center of the newly formed galaxy (Mingarelli 2019), forming an inspiraling binary (Begelman et al. 1980), demonstrated by the simulation in Figure 1. As binaries spiral around each other, the black holes become gravitationally bound due to dynamical friction (Begelman et al. 1980). As two massive accelerating objects spiral around each other, they disrupt space-time, forming waves (Einstein 1920), it is thereby predicted that two spiraling SMBHs emit gravitational waves (Abbott et al. 2016). Research with cosmological simulations seeks to demonstrate the effects of this predicted relationship.

The process in which a binary becomes tightly bound is referred to as hardening (Rozner & Perets 2022). Binary hardening occurs through the combined impact of dynamical friction, gravitational radiation, and gas (Begelman et al. 1980). Each of these three factors dominates in different regimes to the point where the factors can be neglected outside of their own regime (Rozner & Perets 2022). For example, gravitational radiation dominates in the gravitational regime, and the other two factors can safely be ignored. Binary hardening is a key mechanism in binary evolution that shrinks a

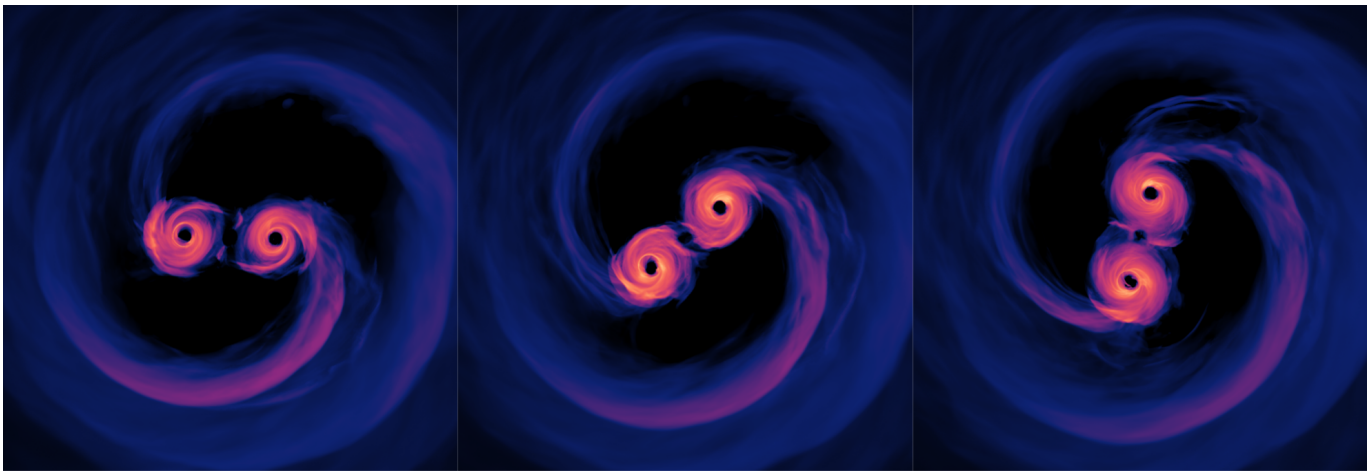

Figure 1: Snapshots of a simulation of the light emitted from a SMBHB merger event (Noble et al. 2018; d'Ascoli et al. 2018)

binary's separation until an eventual merger event. It is while binaries harden in the gravitational regime that it is predicted they are a source of GW.

Pulsars are astrophysical objects that regularly emit pulses of electromagnetic radiation, which can be observed on Earth. Due to their regularity, the time of arrival (TOA) of each pulse can be predicted, but there is often a difference between the predicted TOA and the observed TOA (Lynch 2015). These differences are called pulsar timing residuals. For a circular binary, residuals are predicted to have a sinusoidal variation due to the influence of gravitational waves (Detweiler 1979). Therefore, one can analyze the wave of the residuals to search for and detect a gravitational wave background (GWB) by taking an array of pulsars (Foster & Backer 1990).

The North American Nanohertz Observatory for Gravitational Waves (NANOGrav) is the first group to successfully use pulsar timing arrays (PTAs) to confirm the presence of a GWB (Agazie et al. 2023a). NANOGrav constructed a data set of timing data from 68 pulsars across a 15-year period (Agazie et al. 2023a). They performed a Bayesian statistical analysis in order to measure the strain amplitude of the background. Characteristic GW strain h_c is a dimensionless quantity that characterizes the strength of a GW signal. The power law spectrum used by NANOGrav for the characteristic GW strain is given by Equation 1 (Agazie et al. 2023b). Here, the strain amplitude A_{yr} refers to the magnitude of the GWB signal at a reference frequency of 1 yr^{-1} in the ideal case where

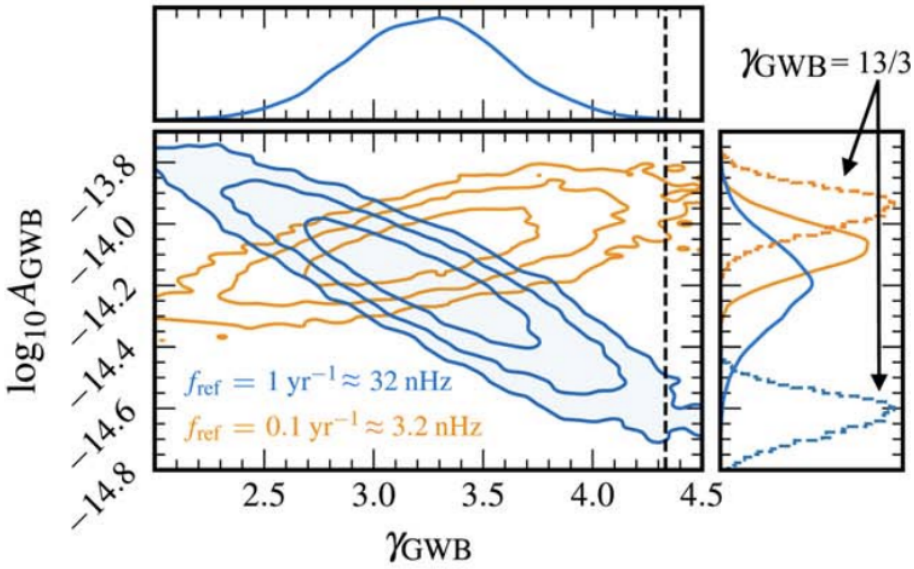

Figure 2: GWB posterior probability distribution from NANOGrav's 15 yr data set (Agazie et al. 2023a).

$\alpha = 2/3$. NANOGrav concluded that the strain amplitude is $2.4^{+0.7}_{-0.6} \times 10^{-15}$ at a 90% confidence interval for a reference frequency of 1 yr^{-1} (Agazie et al. 2023a). This value is consistent with the values expected for a signal caused by SMBHBs (Agazie et al. 2023b); however, as of yet, NANOGrav does not have enough evidence to identify the origin of the signal they detected.

$$h_c(f) = A_{yr} \cdot \left(f/yr^{-1}\right)^{-\alpha} \tag{1}$$

In their analysis, NANOGrav utilized the software ENTERPRISE to analyze pulsar timing and perform gravitational wave searches (Ellis et al. 2020). ENTERPRISE uses Markov chain Monte Carlo methods to constrain the set of samples and create a posterior distribution to approximate the most likely value of a given parameter (Ellis et al. 2020), such as strain amplitude. An example posterior plot produced from an MCMC sampler for strain amplitude is shown in Figure 2.

Previous papers have made other predictions for the GWB amplitude, and one method is to generate a population of SMBHBs from a cosmological hydrodynamic simulation (Agazie et al. 2023b). We have already seen these types of studies with the Millennium simulation (Sesana et al. 2009) and the Illustris simulation. (Kelley et al. 2017). Generating populations using a simulation is useful because,

with pulsar timing data, such as the NANOGrav 15-year data set, we cannot determine the relationship between the data and SMBHs. However, this relationship is known in simulated residuals from simulated populations. So far, ENTERPRISE has not been tested with many simulations, but there is value in testing the software with simulated data in order to gain a more controlled understanding of how the analysis works. We can manipulate the data set in a multitude of ways, testing the effect of specific features of SMBHs on ENTERPRISE, something we cannot do from pulsar timing data. An example of this type of experiment is testing what features of a black hole affect ENTERPRISE's recovered strain amplitude and drawing comparisons with the 15-year result. These types of studies allow us to make inferences about actual SMBH populations in the universe and how they affect gravitational wave emission. This project aims to create a realistic binary population extrapolated from the HR5 simulation that will be used in a variety of future studies with ENTERPRISE.

2. BACKGROUND

2.1. *Horizon Run 5*

HR5 is a cosmological hydrodynamical simulation that can imitate physical processes from a wide range of scaling, from a Gpc to a kpc, at a high resolution (Lee et al. 2021). HR5 models galaxy formation by considering the growth of SMBHBs (Lee et al. 2021). HR5 is yet to be used in GWB detection experiments in the same way Illustris has (Kelley et al. 2017). From Illustris, one can extract SMBHB populations from a redshift starting at $z = 127$ to $z = 0$ (Nelson et al. 2015); in contrast, the HR5 population can only represent redshifts of $z = 200$ to $z = 0.625$ (Lee et al. 2021). Binaries with redshifts greater than 0.625 are over 2300 Mpc away from Earth, so the signal produced by these binaries would be too faint for the current sensitivity of PTAs. The implication of this is that in order to create a realistic population of binaries from the HR5 simulation output, we need to estimate each binary's parameters billions of years later. This process of parameter estimation should produce a population of binaries with lower redshifts.

Using a simulation is beneficial for a number of reasons, including the freedom to control specific features of black holes. With a simulated data set, we have the ability to isolate certain characteristics

and control what we are testing because we know the sources, whereas with pulsar timing data, we only hypothesize the sources. Despite being highly realistic, the data is still simulated. Therefore, we cannot draw definitive conclusions about the origin of gravitational wave backgrounds based on experimentation done with simulated SMBHBs alone. However, the value of these studies comes from developing and testing software with simulated data sets in order to test theories and make inferences, expanding our understanding of the universe.

2.2. *Black Hole Binary Evolution*

SMBHB evolution is the process of a black hole binary from its formation at a galaxy merger to its coalescence. In brief, the life cycle of an SMBHB starts when a galaxy merger brings the two SMBHs close together; as the separation between them continues to decrease, they lose energy, at which point they become gravitationally bound and can be called a binary (Begelman et al. 1980). Different hardening factors, including dynamical friction and gravitational radiation, cause energy loss. The loss of energy causes the binaries to continue to inspiral and harden, shrinking the evolution timescale and separation between the BHs until coalescence (Begelman et al. 1980). A binary is considered coalesced from when its orbit is no longer regarded as stable to when the binary becomes a single body. A binary's lifecycle can be modeled via a series of equations that describe how a binary's separation changes over time in the different hardening regimes. These series of equations are typically called hardening models, often comprising separate formulas for each regime. HOLODECK is a black hole binary population synthesis software that has the capability to predict the parameters of a binary through a process it refers to as *evolving* the binary.

In this paper, modeling binary evolution requires the summation of differential formulas describing the separation of a binary over time in each of the different regimes; these are called the hardening rates in separation. Integrating the hardening rate tells us the separation over a given hardening timescale, and HOLODECK interrupts this process once the binaries coalesce. HOLODECK has the option to use a hardening model with a fixed lifetime, which calculates a hardening rate with a phenomenological functional form and a GW-driven hardening rate where $\frac{da}{dt} = \frac{da_p}{dt} + \frac{da_{GW}}{dt}$ (L. Z. Kelley et al. 2023, in preparation). The Phenomenological function is given by Equation 2, which

depends on a normalization factor A, the binary separation a_p, the characteristic radius r_{char}, and two power law indices g_1 and g_2. The GW-driven formula, given in Equation 3, depends on the separation a_{GW}, the mass of the two BHs m_1 and m_2, the gravitational constant G, the speed of light c, and eccentricity e (L. Z. Kelley et al. 2023, in preparation). Equation 3 is equivalent to Eq. 5.6 in (Peters 1964). Both of these formulas are negative because separation a shrinks as the binaries evolve.

$$\frac{da_p}{dt} = -A * \left(1.0 + \frac{a}{r_{\rm char}}\right)^{(-g_2-1)} / \left(\frac{a}{r_{\rm char}}\right)^{(g_1-1)} \tag{2}$$

$$\frac{da_{GW}}{dt} = \frac{-64}{5} \frac{G^3 m_1 m_2 (m_1+m_2)}{c^5 a^3 (1-e^2)^{7/2}} \left(1 + \frac{73}{24}e^2 + \frac{37}{96}e^4\right) \tag{3}$$

2.3. *Observer-Frame Population*

A simulation only represents a small portion of the universe. Hence, we want to expand our simulated population into a population that would exist in the observer-frame universe. The observer-frame universe is the whole universe from the perspective of the observer in their particular reference frame, and for the rest of the paper, this is referred to as the observer-universe. As such, a binary in this expanded population is referred to as an observer-frame binary. This conversion first entails determining the likelihood that our binaries exist in the observer-universe and then resampling our binary population based on these likelihoods. This scales up the simulation volume, creating more binaries in a larger universe. The scaled-up universe will have a larger population of binaries than the original simulation box.

HOLODECK can perform this expansion after evolution, by first calculating a scale factor that signifies the differential number of binaries in the observer-universe that each binary in the simulated population represents (Kelley et al. 2017). This scale factor calculated with the formula $\Lambda \equiv \frac{1}{V_{sim}} \frac{dV_c}{dz} \frac{dz}{dt} \frac{dt}{dln(f)}$ where Λ is the scale factor, V_{sim} is the volume of the simulation, V_c is the comoving volume, z is redshift, and f is the orbital frequency. This equation is similar to Eq. 15 in (Kelley et al. 2017).

Λ multiplied by an additional factor of $\Delta dln(f)$, finds the weight of each binary. A simulated binary's weight corresponds to the number of binaries in the observer-universe per log orbital frequency interval that is similar to it. This weight is unique for every binary in the simulated data set (L. Z. Kelley et al. 2023, in preparation). Then, HOLODECK uses kernel density estimation to create a new sample of binaries based on the initial values from our population and the weight of each binary. This process constructs a full observer-universe of unique binaries based on our simulated population (L. Z. Kelley et al. 2023, in preparation).

However, there are limitations with HOLODECK's current ability to determine the frequency of each observer-universe binary. While resampling, the binary is ideally interpolated to an entire interval of frequencies. However, HOLODECK is still in development and does not distribute the binaries across the entire chosen frequency interval. For now, HOLODECK assigns the binaries frequencies in a small range around the center of each interval. Hence, it becomes necessary to appropriately distribute the binaries within each frequency interval outside of HOLODECK. Once HOLODECK incorporates this, this step in our methodology will be unneeded in future replications of our experiments.

During evolution, binaries spend a certain amount of time emitting at a frequency within a specific frequency interval (Kelley et al. 2017), implying certain frequencies have more binaries emitting at that frequency than others. This relationship is predicted by a power law with a spectral index of $-8/3$, as found in Equation 4 (Jaffe & Backer 2003). Here, $N(f)$ is the differential number of binaries in the observer-universe in each frequency bin within an interval and f is the frequency. This power law, combined with the weights determined by the scale factor Λ, constructs a population of observer-frame binaries with a realistic distribution of frequencies.

$$N(f)(df/f) \propto f^{-8/3}(df/f) \tag{4}$$

In all, this project is just one step towards more experimentation with GW detection. We aim to diversify the cosmological simulations used for GW detection studies by formulating a system for preparing data sets extracted from HR5. This system evolves the binaries forward in time through

parameter estimation using and expands the population volume to represent the observer-universe. Future research will utilize this paper's results in various manners related to GW detection.

3. METHODS

This work is a continuation of the work done by Hyo Sun Park, who extracted our initial set of binaries from Horizon Run 5. This data set contains the binaries' initial parameters, including the mass of the primary BH m_1, the mass of the secondary BH m_2, the redshift z, comoving distance d_c, luminosity distance d_l, and separation a. HOLODECK considers these initial parameters and estimates each parameter's value at a specified time point; we call this process evolving the binary because it utilizes models that describe how a binary develops over its lifetime.

There are over 35000 binaries in the unevolved HR5 data set, which is too many for HOLODECK to process in a reasonable time frame. So, only the binaries with a total mass greater than 10^8 $M_\odot$ are processed in this paper. This modification reduces the data frame to just under 6000 binaries and is suitable for processing with HOLODECK. After HOLODECK estimates its evolution, we expand the small simulation sample into a whole universe by estimating the number of binaries in the observer-universe each binary in the simulation represents and their associated parameters.

3.1. *Modeling Binary Evolution*

After initializing the population of binaries, we use the `holodeck.evolution.evolution` class to model each binary's evolution until coalescence. This requires two inputs, including the initial parameters of the binaries and a hardening model. We use the `hardening.Fixed_Time_2pl` class, which uses a combination of a fixed time phenomenological function and a GW-driven hardening rate, given by Equations 2 and 3. The characteristic radius r_{char} is uniform for all binaries at 100 PC, and the power law indices g_1 and g_2 are set to -1.0 and $+1.5$, respectively. The normalization constant A is determined via interpolation by determining what value of A produces the desired hardening timescale. We assume all binaries have a circular orbit, therefore the eccentricity e is set to 0. Our primary experiment uses a hardening timescale of 2 Gyr. However, we will also test the effects of varying this timescale from 1 to 6 Gyr.

We then create an evolution instance and evolve the binaries using the method `Evolution.evolve`. This method determines the rate at which each binary evolves from initial separation to coalescence based on the hardening model we specified and stores this information accordingly.

3.2. *Population Resampling*

After evolution, the population is resampled using `Evolution.sample_universe`; in short, this expands our simulation of binaries into a full universe of binaries. This method requires the specification of orbital frequencies at which to sample the population, which occurs by interpolating each binary to the specified frequencies within a chosen hardening timescale and before their redshift reaches zero. HOLODECK performs this by taking the specified target frequencies as interval boundaries, and for now, HOLODECK interpolates each binary to the center of each interval, a process we will improve in Section 3.3. In this experiment, our orbital frequency edges are $[1 \times 10^{-9}, 1 \times 10^{-8}, 1 \times 10^{-7}]$ Hz, and each binary gets interpolated to the centers $[5.5 \times 10^{-9}, 5.5 \times 10^{-8}]$ Hz. We also chose to downsample the resulting population by a factor of 10 due to the lengthy processing time resulting from excluding a downsampling factor; it should be noted that this decision will decrease the GWB, and future work will study the significance of this and resolve the issue. The `sample_universe` method produces binary parameter values in each frequency interval, the weight of each binary, and the sampled binary data.

The weights correspond to the number of binaries in the observer-universe each binary in the simulation represents. The binary parameter values at each frequency interval are the initial binary parameters from our population, except with the frequencies assigned to each frequency interval center. These two outputs are then used to expand the population with `Kalepy.resample()` by constructing a kernel-density estimate of the distribution function that the binary parameter values were sampled and using this function to resample the data. This process requires the number of sample points we want. This value is determined from a Poisson distribution around the sum of the weights and the reflecting boundary conditions, which are the frequency interval edges. This process produces the sampled binary data returned by `Evolution.sample_universe`, leaving us with a data set of observer-frame binaries with the following parameters: total mass, mass ratio, redshift, and

observer-frame orbital frequency. We will refer to this data set as the observer-frame data since it is the set of binaries created from expanding the simulation volume.

3.3. *Distributing Frequencies*

To appropriately distribute the frequencies of the binaries in the data set, we redistributed the frequencies in each interval according to the power law in Equation 4. Taking each interval individually, we establish logarithmic frequency bin sizes with widths of 0.1. Then, we use Equation 4 to solve for the differential number of binaries in each bin $N(f)$. Taking this value we can use the equation $S = \frac{N(f)}{\sum N(f)}$ to calculate a scale factor that represents the fraction of binaries in each bin. Hence, the product of the total number of binaries in the interval and the scale factor for each bin finds the number of binaries in every bin N_b. For our experiment, this needs to be performed twice because we are working with two intervals: $10^{-9} < f < 10^{-8}$ Hz and $10^{-8} < f < 10^{-7}$ Hz.

Because the scale factor is a non-integer, N_b must be rounded to the nearest integer because we cannot have a fraction of a binary in a bin. A limitation of this process is that the size of both frequency intervals will no longer equal the size of the observer-frame data set.

From here, we know the number of binaries within each logarithmic frequency bin, but not the specific frequency of each binary. To determine this, we uniformly distribute random frequencies to each binary within each bin. Hence, the overall trend across both intervals follows the power law in Equation 4; however, there is a uniform distribution within each bin.

The next step is to convert these frequencies from log space and randomly assign them to a binary in the corresponding frequency interval. Due to our rounding limitation, we will have a small number of binaries without a frequency, and these will be dropped from our data set. Now that we have appropriately distributed frequencies, we can calculate the period and use Kepler's law to find the separation of each binary. Together, these form a data frame of binaries in the observer-universe with a realistic distribution of frequencies.

4. RESULTS

After evolving our original data set of HR5 binaries by using the HOLODECK software, we are left with a universe of observer-frame binaries. There are roughly 400,000 binaries in this set, each with a unique mass, mass ratio, and redshift over a wide range. The frequencies of these binaries were determined outside HOLODECK according to the power law in Equation 4.

4.1. *Frequency Distribution*

The redistribution of frequencies in each interval by the power law in Equation 4 is summarized in Figure 3. Here, the colors correspond to the two frequency intervals: grey for $1 < f < 10$ nHz and blue for $10 < f < 100$. The intervals are labeled based on their interval center, which for the first interval is 5.5 nHz and 55 nHz for the second. Figure 3 shows a right-skewed histogram with

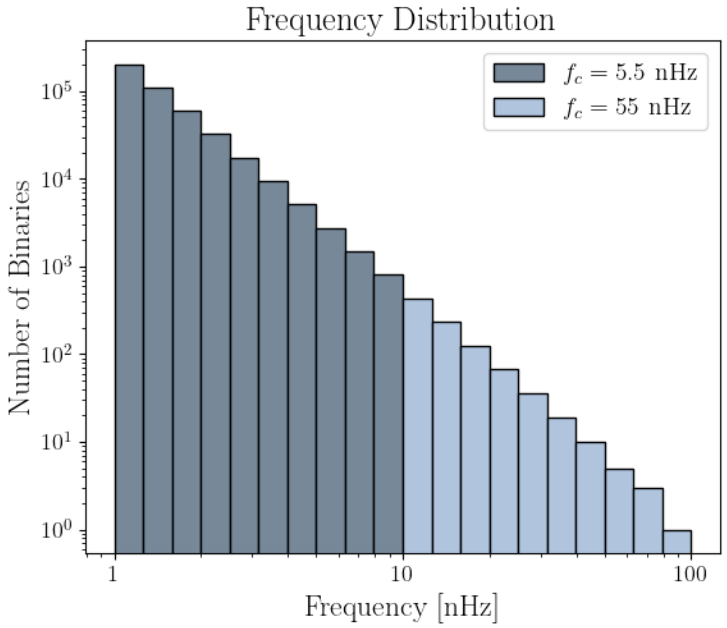

Figure 3: Histogram presenting the results of distributing frequencies according to a power law with a spectral index of $-8/3$. Both axes are on a logarithmic scale. The two colors signify the frequency interval center f_c at which the frequency was originally interpolated to by HOLODECK. The frequencies are given in nanohertz for simplicity.

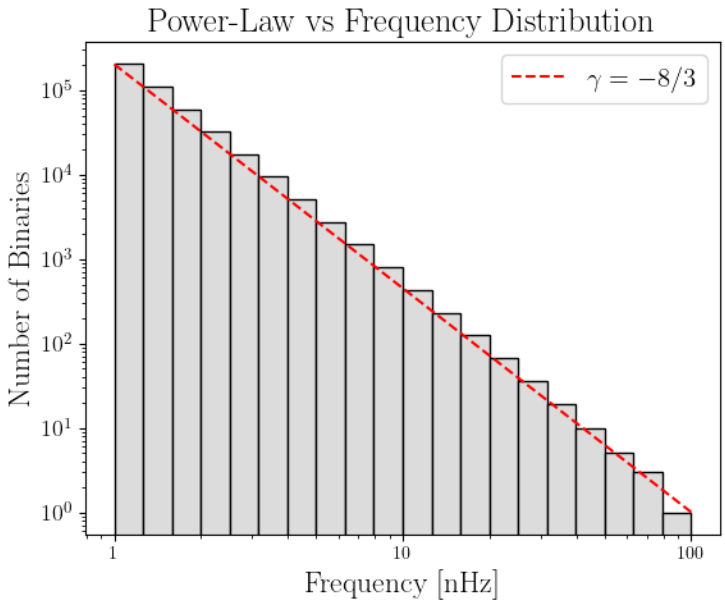

Figure 4: An alternate way to present Figure 3, highlighting the accuracy of our distribution to the expected power law with a spectral index $\gamma = -8/3$. Both axes are on a logarithmic scale.

nearly half of the data set lying in the first bin. The spread of the data is as expected, with its range spanning $1 < f < 95$ nHz, covering both of the target intervals.

Each interval in the observer-frame data set was distributed separately according to the power law in Equation 4, but the combined set of each interval should still abide by the power law. Figure 4 illustrates that the combined data set abides as expected, indicating our methodology for distribution was accurate. In log space, the power law given in Equation 4 appears as a line with a slope equivalent to the spectral index $\gamma = -8/3$. As seen in Figure 4, the slope of the histogram, which is the rate of change of the height of each bin, equals the expected value of $-8/3$.

4.1.1. *Hardening Timescale Analysis*

The previous results evolved the binaries with a hardening timescale of 2 Gyr. The results of testing our process with a range of hardening timescales (1-6 Gyr) are summarized in Figure 5. What is notable about this result is that a longer timescale results in fewer binaries per frequency bin. Hence, there is also a decline in the number of binaries in the observer-universe for the increasing timescale, as Table 1 outlines. This is likely due to fewer binaries reaching the target frequencies before the

redshift reaches zero during evolution. Moreover, there is an effect where the volume of the universe gets larger for higher redshifts (Kelley 2024). In our populations, the binaries evolved at smaller timescales tend to have higher redshifts and larger volumes, which is consistent with this effect.

Table 1: Summary of observer-universe for each timescale

Timescale (Gyr)	Number of Binaries	Redshift
1	5.3×10^5	$0.38 < z < 2.4$
2	4.4×10^5	$0.28 < z < 1.9$
3	3.5×10^5	$0.20 < z < 1.4$
6	1.1×10^5	$0.0048 < z < 0.7$

We also replicated the histogram in Figure 3 for each new population. At these timescales, the slope of each histogram remains equal to the expected value of $-8/3$. This shows that there is not a significant reduction in accuracy for our process of frequency redistribution with varied hardening timescales. However, we do notice that the spread of the data is more limited for larger hardening timescales. For instance, as seen in Figure 5, for $t = 6$ Gyr, the frequencies all reside in the range $1 < f < 64$ nHz where we would expect the upper bound to be around 100 nHz. This is due to the populations evolved at larger hardening timescales having smaller volumes, as previously explained.

4.2. *Final Population*

Table 2, located in the appendix, summarizes the random assignment of each binary in the original HR5 data set a new frequency based on the distribution in Figure 3. Each binary now has a new frequency in the same interval it interpolated to in HOLODECK. This is the completed, evolved

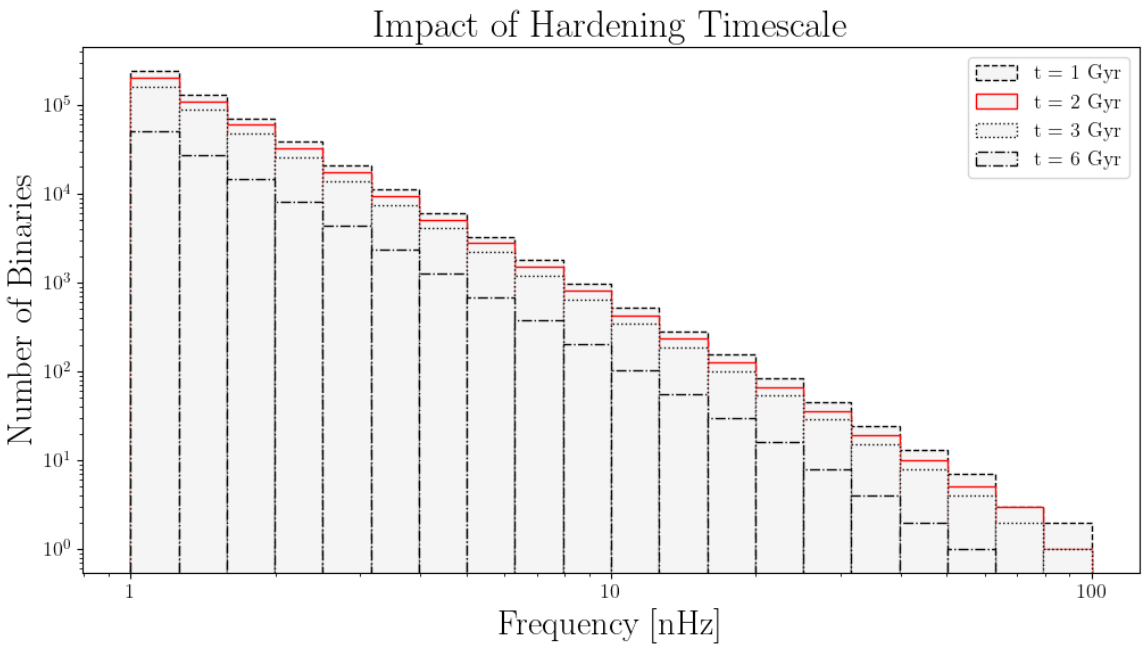

Figure 5: Overlaid histograms displaying the results of testing the effect of the hardening timescale on HOLODECK's binary evolution. Red represents a timescale of 2 Gyr, which is the same population in Figure 3 and 4.

observer-frame data set that is prepared to be used for simulated pulsar timing analysis and GWB detection.

Two of our parameters were unaffected by our frequency redistribution which were mass and redshift. This research limited its scope by only analyzing SMBHBs with high masses, $M_\bullet > 10^8 M_\odot$. The full distribution of the total mass M_{tot} in the data set is shown in Figure 6; this histogram is right-skewed with over 80% of the data set falling in the first bin. The colors serve the same purpose as they did in Figure 3. The masses of the binaries in the first interval all fall in the range $7.1 \times 10^7 < M_{tot} < 3.8 \times 10^9\ M_\odot$. The masses of the binaries in the second interval all fall in the range $8.2 \times 10^7 < M_{tot} < 7.9 \times 10^8\ M_\odot$.

Figure 7 depicts the distribution of redshift among our binaries. Around 67% of the binaries have a redshift in the range $0.625 < z < 1.25$. Additionally, the total range of redshifts in the data set is $0.28 < z < 1.91$. Before our evolution model, the minimum redshift determined by HR5 was 0.625,

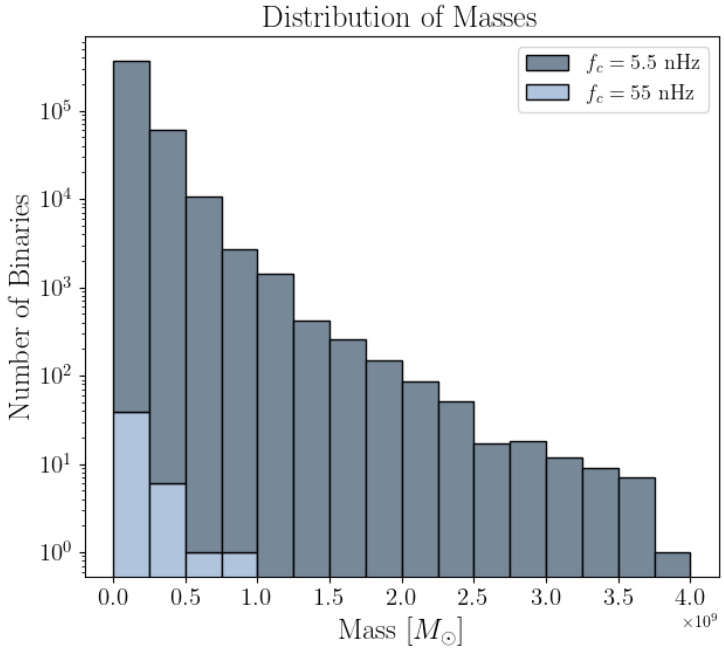

Figure 6: Stacked histogram displaying the distribution of total mass across the data in Table 2. These masses were determined by the sampling completed by HOLODECK. The two colors signify the frequency interval center f_c at which the frequency was originally sampled at by HOLODECK.

which was too distant for GW detection. However, with our model, we have successfully developed a data set of simulated binaries with low redshifts that are more suitable for detection. There are approximately 10^5 binaries that have $z < 0.625$ and are good candidates for future studies.

Other known properties of these binaries are their separation and period, which are affected by our frequency redistribution. The separation of each binary is calculated using Kepler's law; Figure 8 displays the distribution of separations among our binaries, which has a slight right skew. Around 67% of the binaries have a separation between $0.015 < a < 0.025$ pc. However, the total range of separation is $0.0014 < a < 0.073$ pc. For comparison, the range of separations originally extracted from HR5 for these binaries was $41 < a < 194221$ pc, demonstrating how significantly a binary hardens during this process.

Our final parameter to analyze is the orbital period T. The orbital period of a binary is dependent on the frequency by the relationship $T = 1/f$; therefore, is affected by our distribution summarized in

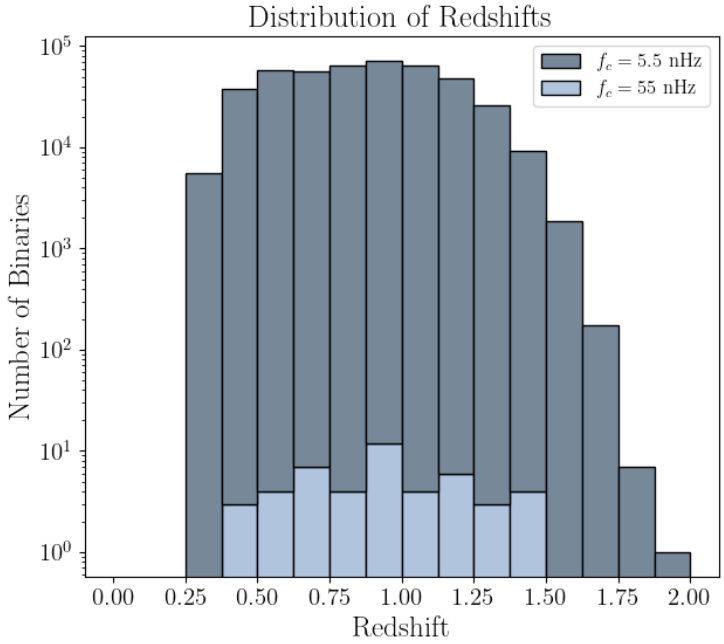

Figure 7: Stacked histogram displaying the distribution of redshift z across the data in Table 2. These redshifts were determined by the sampling completed by HOLODECK. The two colors signify the frequency interval center f_c at which the frequency was originally sampled at by HOLODECK.

Figures 3 and 4. Figure 9 displays the distribution of periods amongst our data set. This distribution is left-skewed, with most of the population having a period greater than 24 years. For a GW to be detectable, the Nyquist theorem suggests binaries with too large an orbital period will not produce a detectable GW. Current estimates suggest our binaries need to have a period shorter than 20 years. Nearly 30% of the binaries meet this criterion ($T < 20$).

Our experiments successfully created a population that is suitable for use in studies analyzing simulated gravitational wave signals, as nearly 30,000 binaries have both a redshift lower than 0.625 and a period shorter than 20 years. These results are a promising step towards GW detection using the HR5 simulation.

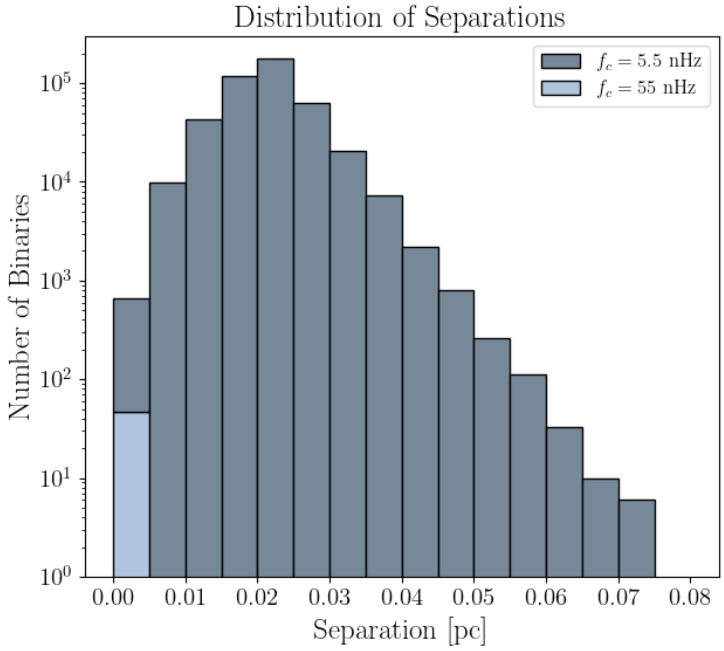

Figure 8: Stacked histogram displaying the distribution of separation a across the data in Table 2. These separations were determined by the sampling completed by HOLODECK. The two colors signify the frequency interval center f_c at which the frequency was originally sampled at by HOLODECK.

5. DISCUSSION

5.1. *Conclusion*

The foundation of the project is to model the evolution of a supermassive black hole binary population in order to develop a simulated data set representative of the observer-universe that has parameters suitable for gravitational wave simulations. There are multiple factors that make the simulated data set suitable, including having low redshifts and a short period. As it was, the extracted HR5 simulated population did not meet this definition of suitable, so we developed the population by modeling each binary's evolution and expanding the population. Our methodology was successful in creating a population of binaries with these necessary parameters.

What makes this data set suitable is that the binaries have redshifts as close to $z = 0$ as possible. A limitation of the Horizon Run 5 simulation is that it can only simulate a population with redshifts greater than 0.625, whereas other cosmological simulations used for this type of research, like the

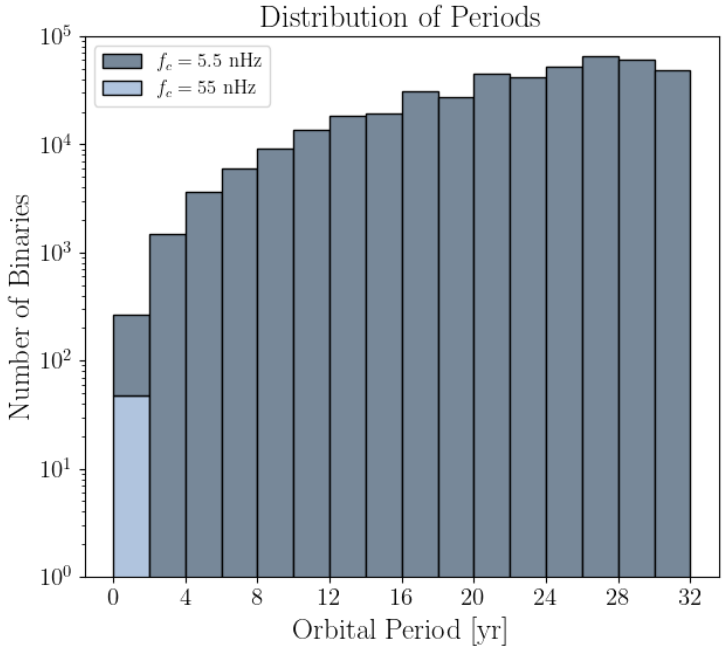

Figure 9: Stacked histogram displaying the distribution of periods across the data in Table 2. These periods were determined by the orbital frequencies after redistribution. The two colors signify the frequency interval center f_c at which the frequency was originally sampled at by HOLODECK.

Illustris simulation, can simulate binaries with redshifts as low as $z = 0$. Binaries with $z = 0.625$ are nearly 2300 Mpc away from Earth and would produce a signal too faint to be detectable. This study was successful in forming a population of binaries where over 10^5 binaries have $z < 0.625$. Another constraint is that binaries with orbital periods longer than 20 years will not simulate a detectable GWB. In our population, over 1.29×10^5 binaries have a period shorter than 20 years. In all, there are 2.9×10^4 binaries with both $z < 0.625$ and $T < 20$. This means that we have a sufficiently large data set with enough binaries meeting both criteria. Thus, we expect this dataset to be comparable to other populations of binaries extracted from the Illustris simulation and be able to simulate a detectable signal. Our findings provide us with a promising start for future GW detection experiments with this new population.

5.2. *Future Work*

The methodology laid out in this paper is easily reproducible, and the results in Table 2 are just an example of one population of binaries that can be developed from the HR5 data set. Due to the random sampling involved with the expansion of the simulation, different iterations of binaries can easily be produced. These simulated populations will be used to further test and analyze ENTERPRISE, creating a controllable environment to test the software. Unlike with pulsar timing data, we can control specific features (binary parameters, noise, etc) and analyze their effect on ENTERPRISE, directly viewing the relationship between SMBHs and GWs, allowing us to make inferences about the activity of SMBHs in the universe.

Though there are a few studies done on the detection of GWs using cosmological simulations, none have used Horizon Run 5. Our findings will serve as the basis for future studies on GW detection using the population produced by HR5.

6. ACKNOWLEDGMENTS

This research was supported and advised by Dr. Andrea Lommen and done in close collaboration with Claire Jones. I would also like to thank the NANOGrav team for their support and Dr. Luke Zoltan Kelley for his guidance while using HOLODECK.

REFERENCES

Abbott, B. P., et al. 2016, Phys. Rev. Lett., 116, 061102, doi: 10.1103/PhysRevLett.116.061102

Agazie, G., et al. 2023a, The Astrophysical Journal Letters, 951, L8, doi: 10.3847/2041-8213/acdac6

—. 2023b, The Astrophysical Journal Letters, 952, L37, doi: 10.3847/2041-8213/ace18b

Begelman, M. C., Blandford, R. D., & Rees, M. J. 1980, Nature, 287, 307, doi: 10.1038/287307a0

Detweiler, S. 1979, Astrophys. J., 234, 1100

d'Ascoli, S., Noble, S. C., Bowen, D. B., et al. 2018, The Astrophysical Journal, 865, 140, doi: 10.3847/1538-4357/aad8b4

Einstein, A. 1920, The Generalized Principle of Relativity (The University of Calcutta), 89–163

Ellis, J. A., Vallisneri, M., Taylor, S. R., & Baker, P. T. 2020, ENTERPRISE: Enhanced Numerical Toolbox Enabling a Robust PulsaR Inference SuitE, Zenodo

Foster, R. S., & Backer, D. C. 1990, Astrophys. J., 361, 300

Ghez, A. M., Klein, B. L., Morris, M., & Becklin, E. E. 1998, The Astrophysical Journal, 509, 678, doi: 10.1086/306528

Jaffe, A. H., & Backer, D. C. 2003, The Astrophysical Journal, 583, 616, doi: 10.1086/345443

Kelley, L. Z. 2024, personal communication

Kelley, L. Z., Blecha, L., Hernquist, L., Sesana, A., & Taylor, S. R. 2017, Monthly Notices of the Royal Astronomical Society, 471, 4508–4526, doi: 10.1093/mnras/stx1638

Lee, J., Shin, J., Snaith, O. N., et al. 2021, The Astrophysical Journal, 908, 11, doi: 10.3847/1538-4357/abd08b

Lynch, R. S. 2015, Journal of Physics: Conference Series, 610, 012017, doi: 10.1088/1742-6596/610/1/012017

Mingarelli, C. M. F. 2019, Nature Astronomy, 3, 8–10, doi: 10.1038/s41550-018-0666-y

Nelson, D., Pillepich, A., Genel, S., et al. 2015, Astronomy and Computing, 13, 12–37, doi: 10.1016/j.ascom.2015.09.003

Noble, S., Kazmierczak, J., & Wiessinger, S. 2018, Supermassive Black Hole Binary Simulation Visualizations in 4k, NASA. https://svs.gsfc.nasa.gov/13086

Peters, P. C. 1964, Phys. Rev., 136, B1224, doi: 10.1103/PhysRev.136.B1224

Rozner, M., & Perets, H. B. 2022, The Astrophysical Journal, 931, 149, doi: 10.3847/1538-4357/ac6d55

Sesana, A., Vecchio, A., & Volonteri, M. 2009, Monthly Notices of the Royal Astronomical Society, 394, 2255–2265, doi: 10.1111/j.1365-2966.2009.14499.x

Sobolenko, M., Berczik, P., & Spurzem, R. 2021, AA, 652, A134, doi: 10.1051/0004-6361/202039859

APPENDIX

Table 2: Summary of Simulated Binary Parameters

Total Mass ($M_\odot$)	Primary Mass ($M_\odot$)	Secondary Mass ($M_\odot$)	Mass Ratio	Separation (pc)	Redshift	Frequency (Hz)	Period (yr)
2.81E+08	2.80E+08	6.47E+05	0.0023	0.0016	1.187	9.26E-08	0.34
1.43E+08	1.40E+08	2.85E+06	0.0203	0.0014	0.605	7.64E-08	0.41
4.30E+08	4.23E+08	7.09E+06	0.0168	0.0023	0.634	6.37E-08	0.50
3.80E+08	3.79E+08	8.24E+05	0.0022	0.0022	0.398	6.37E-08	0.50
1.08E+08	1.06E+08	1.39E+06	0.0131	0.0017	1.102	5.13E-08	0.62
1.94E+08	1.93E+08	7.07E+05	0.0037	0.002	0.515	5.41E-08	0.59
1.54E+08	1.34E+08	1.97E+07	0.1472	0.0018	1.429	5.33E-08	0.59
7.88E+08	7.87E+08	1.24E+06	0.0016	0.0029	0.91	5.98E-08	0.53
9.44E+07	9.02E+07	4.19E+06	0.0464	0.0016	1.449	5.36E-08	0.59
4.42E+08	4.40E+08	1.63E+06	0.0037	0.0028	0.675	4.89E-08	0.65
1.22E+08	1.18E+08	4.13E+06	0.0351	0.022	0.824	1.15E-09	27.57
1.39E+08	9.38E+07	4.50E+07	0.4802	0.0221	0.585	1.22E-09	25.99
1.97E+08	1.84E+08	1.32E+07	0.0719	0.0244	0.804	1.24E-09	25.57
2.30E+08	1.91E+08	3.85E+07	0.2015	0.0277	0.411	1.11E-09	28.56
1.80E+08	1.60E+08	1.95E+07	0.1219	0.0268	0.646	1.03E-09	30.78
1.23E+08	1.22E+08	1.52E+06	0.0125	0.0217	1.071	1.17E-09	27.10
1.49E+08	1.48E+08	6.52E+05	0.0044	0.0233	0.787	1.16E-09	27.33
9.14E+07	8.90E+07	2.46E+06	0.0277	0.0209	0.942	1.07E-09	29.63
1.12E+08	1.09E+08	3.15E+06	0.0289	0.0233	0.924	1.01E-09	31.39
1.30E+08	1.29E+08	7.10E+05	0.0055	0.0223	0.965	1.15E-09	27.57

NOTE—Full Detectable Data Set is available on Github